Optical Weak Link between Two Spatially Separated Bose-Einstein Condensates

Y. Shin, G.-B. Jo, M. Saba, T. A. Pasquini, W. Ketterle, and D. E. Pritchard*

Department of Physics, MIT-Harvard Center for Ultracold Atoms, and Research Laboratory of Electronics,
Massachusetts Institute of Technology, Cambridge, Massachusetts, 02139, USA
(Received 6 July 2005; published 17 October 2005)

Two spatially separate Bose-Einstein condensates were prepared in an optical double-well potential. A bidirectional coupling between the two condensates was established by two pairs of Bragg beams which continuously outcoupled atoms in opposite directions. The atomic currents induced by the optical coupling depend on the relative phase of the two condensates and on an additional controllable coupling phase. This was observed through symmetric and antisymmetric correlations between the two outcoupled atom fluxes. A Josephson optical coupling of two condensates in a ring geometry is proposed. The continuous outcoupling method was used to monitor slow relative motions of two elongated condensates and characterize the trapping potential.

Josephson effects [1] are quantum phenomena in which the current between two weakly coupled, macroscopic quantum systems depends on the relative phase of the two systems. These effects are direct evidence for the existence of the phase of a macroscopic quantum system [2] and observed in quantum systems such as superconductors [3], superfluid ^{3}He [4], and Bose condensed gases [5,6]. Josephson coupling between two systems is typically established via tunneling through a separating potential barrier or via an external driving field as in the internal Josephson effect [7,8]. Both couplings require spatial overlap of the two systems due to the intrinsic locality of the coupling interactions.

The concept of Josephson coupling can be extended to include two *spatially separate* quantum systems by using intermediate coupling systems. If the phase relations among these systems are preserved and thus the net particle exchange is phase sensitive, the two spatially separate systems might be regarded as being effectively Josephson coupled via the intermediate systems. Furthermore, the phase of the coupling may be actively controlled by adjusting the coupling states of the intermediate systems. This idea has been theoretically introduced in the context of relative phase measurement [9].

In this Letter, we experimentally demonstrate phase-sensitive optical coupling of two spatially separate Bose-Einstein condensates using Bragg scattering. The situation we are investigating is two condensates, irradiated by two pairs of Bragg beams [Fig. 1(a)]. The two pairs of Bragg beams couple out beams of atoms propagating to the left or the right, respectively, and these unconfined propagating atoms constitute the intermediate coupling system in our scheme. Depending on the relative phases of the two condensates and the coupling states, we observe only one outcoupled beam propagating to one or the other side, or two identical beams propagating in opposite directions (Fig. 2). This demonstrates phase control of currents and establishes a new scheme to realize Josephson effects with two nonoverlapping condensates. In the following, we

present a model for the phase-sensitive outcoupling process and an experimental test of the prediction that the phase of the atomic currents into each condensate can be controlled. Finally, we suggest a Josephson optical coupling of two condensates in a ring geometry.

First, we elaborate on the situation with a unidirectional optical coupling [Fig. 1(b)]. We use the conventional wave function description for condensates. Two condensates 1 and 2 are trapped in a double-well potential and optically coupled into unconfined states by a single pair of Bragg beams. Ignoring the accumulated phase shifts due to the interaction with the condensates, we approximate the unconfined coupling states as truncated free propagating states, i.e., $\psi_i(x, t) \propto \Theta(x - x_i)\sqrt{\gamma N_i}e^{i\chi_i(x,t)}$ $(i = 1, 2)$, where $\Theta(x)$ is the Heaviside step function, γ is the outcoupling efficiency of the Bragg beams, N_i is the total atom
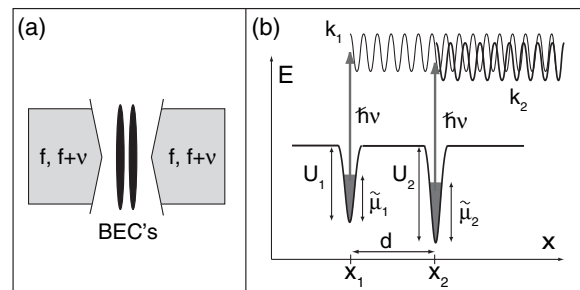

FIG. 1. Optical coupling between two separate condensates. (a) Bidirectional coupling. Two pairs of Bragg beams with frequencies f and $f + \nu$ are applied to two separate condensates. (b) Outcoupling process. Two condensates are trapped at $x = x_1$ and x_2 $(d = x_2 - x_1)$. A pair of Bragg beams with frequency difference ν generate a continuous atomic beam from each condensate. The two atomic beams overlap in $x > x_2$, forming a matter wave interference pattern. U_1 (U_2) denotes the trap depth of the left (right) well, $\tilde{\mu}_1$ $(\tilde{\mu}_2)$ the mean-field interaction energy of the left (right) condensate, and k_1 (k_2) the wave number of the atomic beam from the left (right) condensate outside the trap.
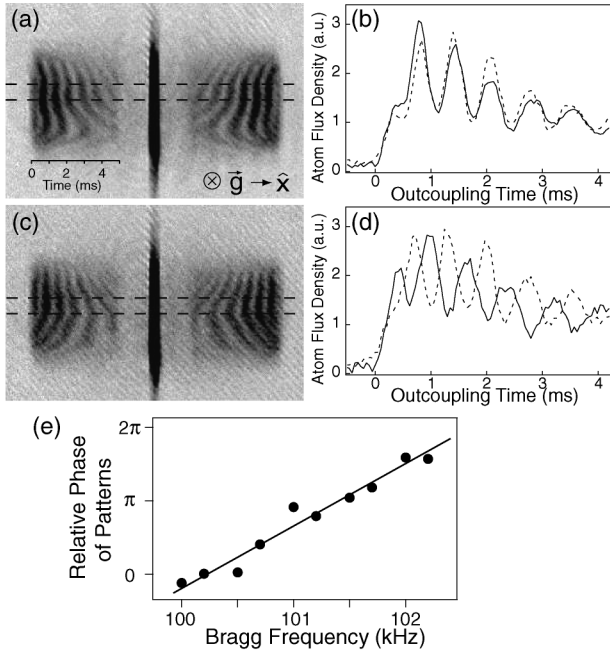
FIG. 2. Symmetric and antisymmetric correlation between out-coupled atom patterns. Two pairs of Bragg beams [Fig. 1(a)] outcoupled atoms in either $+x$ or $-x$ direction. Absorption images were taken after 5 ms outcoupling and 2 ms additional ballistic expansion. The left outcoupled atom patterns were compared with the corresponding right patterns. Symmetric correlation between two patterns was observed at (a) $\nu = 2\pi \times 100.5$ kHz and (c) antisymmetric at $\nu = 2\pi \times 101.5$ kHz. The field of view is $900 \ \mu\text{m} \times 590 \ \mu\text{m}$. (b), (d) Outcoupled atom flux densities were obtained by integrating optical densities between the dashed lines and converting the spatial coordinate to the time coordinate. The solid (dashed) lines correspond to left (right) outcoupled atoms. (e) The coupling phase θ of the two outcoupled patterns showed a linear dependence on ν with $\partial\theta/\partial\nu = (2.4 \text{ kHz})^{-1}$.

number of condensate i, and $\chi_i(x, t) = k_i x - \omega_i t + \chi_{i0}$ is the phase of the coupling state with $\hbar\omega_i = \frac{\hbar^2 k_i^2}{2m}$, where m is atomic mass. The phase continuity at the coupling position $x = x_i$ requires

$$\chi_i(x_i, t) = \phi_i(t) + \phi_B(x_i, t) - \pi/2, \quad (1)$$

where $\phi_i(t)$ is the phase of the condensate, $\phi_B(x, t) = 2k_r x - \nu t + \phi_{B0}$ is the phase of the Bragg beams with wave number k_r and frequency difference ν, and $-\pi/2$ is the phase shift attributed to the scattering process [10]. In a linear regime with $\gamma \ll 1$, ϕ_i is not perturbed by the coupling, i.e., $\phi_i(t) = -\frac{\mu_i}{\hbar}t + \phi_{i0}$, where $\hbar$ is Planck's constant divided by 2π and $\mu_i = -U_i + \tilde{\mu}_i$ [Fig. 1(b)] is the chemical potential of the condensate. Satisfying the phase relation Eq. (1) at all t requires

$$\hbar\omega_i = \hbar\nu + \mu_i, \quad (2)$$

$$\chi_{i0} = -\delta k_i x_i + \phi_{B0} + \phi_{i0} - \pi/2, \quad (3)$$

where $\delta k_i = k_i - 2k_r$. Equation (2), the temporal part in Eq. (1), corresponds to energy conservation.

In the overlapping region, $x > x_2$, the two atomic beams from each condensate form a matter wave interference pattern, and the outcoupled atom density $n(x, t) = |\psi_1(x, t) + \psi_2(x, t)|^2$. For a better interpretation, we define the right outcoupled atom density $n_R(s, t) \equiv n(s + x_2, t)$, where s indicates the distance from the right condensate,

$$n_R(s, t) = \frac{\gamma}{2v_r}\left(N_t + 2\sqrt{N_1 N_2} \cos[\Delta k s + \phi_r(t) - \delta k_1 d]\right), \quad (4)$$

where $N_t = N_1 + N_2$, $\Delta k = k_2 - k_1$, $d = x_2 - x_1$, and $\phi_r(t) = \phi_2(t) - \phi_1(t)$. We approximate the propagating velocity $v_i = \frac{\hbar k_i}{2m} \simeq 2v_r$ with $\delta k_i \ll 2k_r$, where $v_r = \frac{\hbar k_r}{m}$ is the recoil velocity. According to the relative phase ϕ_r, outcoupled atoms from the left condensate are coupled into or amplified by the right condensate. The spatial and temporal modulation of the outcoupled atom flux n_R represents the evolution of the relative phase ϕ_r, which was directly demonstrated in our previous experiments [11].

The phase term $-\delta k_1 d$ can be interpreted as the phase shift which outcoupled atoms would accumulate during the flight from the left condensate to the right with respect to the Bragg beam phase ϕ_B which is acting as the phase reference. A similar relation between n_R and ϕ_r can be obtained in terms of the dynamic structure factor of 2 separate condensates [12], but the phase modulation of coupling states in the middle of two condensates is likely to be ignored in the conventional impulse approximation [13]. This phase shift is the key element for an actively controlled optical coupling and its physical importance will be manifest in the following bidirectional coupling scheme.

We now add another pair of Bragg beams to outcouple atoms in the $-x$ direction. Modifying the above calculation by $k_{i,r} \rightarrow -k_{i,r}$, the left outcoupled atom density $n_L(s, t) \equiv n(x_1 - s)$ is given as

$$n_L(s, t) = \frac{\gamma}{2v_r}\left(N_t + 2\sqrt{N_1 N_2} \cos[\Delta k s + \phi_r(t) + \delta k_2 d]\right). \quad (5)$$

Considering the atom flux for each condensate, we find rate equations for N_1 and N_2. For example, the left condensate has influx of γN_2 from the right condensate and outflux of γN_1 and $n_L(0, t)$ in $+x$ and $-x$ direction, respectively. The final rate equations read

$$\dot{N}_{1,2} = -2\gamma\left(N_{1,2} + \sqrt{N_1 N_2} \cos[\phi_r(t) \mp \delta k_{1,2} d]\right). \quad (6)$$

Except for the global depletion effect of Bragg scattering, the rate equations describe Josephson oscillations due to the bidirectional optical coupling, i.e., that the atomic currents into the condensates depend on the relative phase.

The optical Josephson coupling has a unique feature in the control of the phase accumulated by atoms in the

coupling state [9]. Since the intermediate system "delivers" the phase information from one condensate to the other, the phase can be manipulated in transit and consequently, the phase of the effective coupling can be controlled without affecting the two condensates. In the bidirectional coupling scheme, the control of the coupling phase is embodied in the phase shift terms, $-\delta k_1 d$ and $\delta k_2 d$. We define the coupling phase as $\theta \equiv (\delta k_1 + \delta k_2)d$, and with $\delta k_i \ll 2k_r$, approximate θ as

$$\theta = \frac{d}{v_r}\left(\nu - \frac{4E_r}{\hbar} + \frac{\mu_1 + \mu_2}{2\hbar}\right), \qquad (7)$$

where $E_r = \frac{\hbar^2 k_r^2}{2m}$ is the recoil energy. θ is equivalent to the relative phase of n_L and n_R. When $\theta = 0$ ($\theta = \pi$) (mod 2π), n_L and n_R will show (anti)symmetric correlation.

The control of the coupling phase θ was experimentally demonstrated. Condensates of ^{23}Na atoms in the $|F = 1, m_F = -1\rangle$ state were prepared in an optical double-well potential as described in Ref. [14]. The $1/e^2$-intensity radius of a focused laser beam for a single well was 7.6 μm and the typical trap depth was $U_{1,2} \sim h \times 18$ kHz. The separation of the two wells was $d = 11.4$ μm and each well started with a condensate of $\sim 5 \times 10^5$ atoms. Two pairs of Bragg beams parallel to the separation direction were applied to the condensates by retroreflecting two copropagating laser beams with frequency difference ν. The lifetime of condensates was over 18 s. The $1/e$ depletion time due to Bragg scattering into both directions was 4.5 ms, resulting in the magnitude of initial atom currents $\sim 1.1 \times 10^8$ atoms/s. Outcoupling patterns were measured by taking absorption images of outcoupled atoms.

When the Bragg frequency difference ν was varied, the outcoupling pattern cycled through symmetric and antisymmetric correlations (Fig. 2). The coupling phase θ was fit to the observed patterns for each Bragg frequency [Fig. 2(e)]. The linear dependence was measured as $\partial\theta/\partial\nu = (2.4 \pm 0.2 \text{ kHz})^{-1}$, which is consistent with the predicted value $d/v_r = (2.6 \text{ kHz})^{-1}$. This clearly demonstrates the presence and control of the coupling phase in our optical coupling scheme. With the antisymmetric condition, $\theta = \pi$, as a function of the propagating relative phase, the output oscillated between predominantly to the left and predominantly to the right [Figs. 2(c) and 2(d)]. The experimental situation has perfect mirror symmetry. Unidirectional output in a symmetric situation is a macroscopic consequence of the condensates' phase.

Control of the coupling phase can be used to introduce temporal and spatial variations of Josephson-type coupling. Temporal control with real-time feedback could ensure the coherent and continuous replenishment of a condensate [see Ref. [15]]. For elongated condensates, as used here, spatial control with barrier heights or well separations could create spatially varying coupling along the condensate axis, and realize, e.g., ring currents.

One limitation of the bidirectional coupling scheme is that atoms are depleted out of the system due to the linear geometry. Even though the pattern of outcoupled atoms is a crucial signal for monitoring the coupling dynamics, the coupling time is fundamentally limited. To overcome this shortcoming, we envisage a system preserving total atom number like in Fig. 3, where atoms circulate between two condensates in a ring waveguide. With assumptions that the traveling time δt for atoms from one condensate to the other is short enough to satisfy $\dot{\phi}_r \delta t \ll 1$ and that the density profiles are constant over the trajectories between the two condensates, the governing equation, in a linear regime, is

$$\dot{N}_2 - \dot{N}_1 = 2\gamma\sqrt{N_1 N_2}\cos(\phi_r - \phi_m), \qquad (8)$$

where ϕ_m is the effective coupling phase which is determined by the accumulated phase shift over the round trajectories and the phase of the Bragg beams.

The long condensates used here introduce a new degree of freedom into the usual pointlike Josephson junctions: the condensates can have a spatially varying phase along the axial direction. Since the optical coupling is selectively established between condensates at the same axial position, axial gradients of the relative phase are directly observed through tilted fringes in the pattern of outcoupled atoms. In Fig. 4, we present two examples showing the effects of relative dipole and quadruple axial motions of two condensates. Josephson vortex [16] and modulational instabilities [17] in elongated coupled condensates were theoretically suggested.

Continuous Bragg scattering was used to characterize the trap depth and the trap frequency of a single optical trap (Fig. 5). Since momentum and energy imparted in the scattering process are precisely defined, the kinetic energy of atoms coupled out of a trap determines the depth of the trap. We measured the traveling distance D of outcoupled atoms with fixed traveling time t, and determined the trap depth U from the relation, $D/t = \sqrt{4v_r^2 - 2U/m}$, ignoring the mean-field interaction with the condensate and the finite size of the trap. Additionally, the exact knowledge
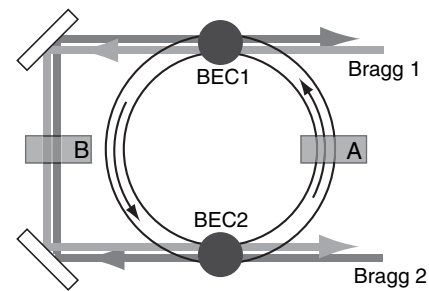

FIG. 3. Optical coupling of two condensates on a ring. Two condensates are confined at opposite sides on a ring-shaped waveguide and a pair of Bragg beams (Bragg 1 and 2) outcouple atoms in the clockwise direction. The shaded boxes A and B are phase modulators for atoms and photons, respectively.
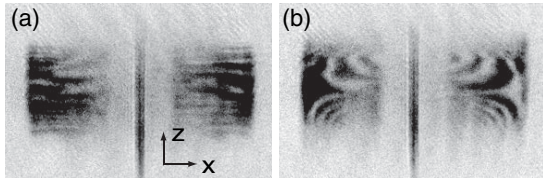
FIG. 4. Monitoring of slow relative axial motions. Two chemical potentials were equalized within 400 Hz and the temporal evolution of the relative phase of two condensates along the axial (z) direction was recorded in the outcoupled atom patterns. (a) represents relative dipole oscillation, corresponding to relative velocity ≈ 300 μm/s or kinetic energy of ≈ 130 pK $\times k_B$, and (b) relative quadruple oscillation. k_B is the Boltzmann constant.

of the recoil velocity v_r calibrates the optical magnification of images.

On the other hand, the trap frequency was measured using velocity sensitivity of Bragg scattering. When a condensate oscillates in a trap, atoms are coupled out only when the condensate is at the resonant velocity. Since the dipole oscillation of a condensate in a harmonic trap is the same as the trap frequency f, the outcoupling frequency is the same as f when Bragg beams are tuned at the maximum velocity [Fig. 5(b)], $2f$ at zero velocity [Fig. 5(c)]. Even though the frequency resolution is limited by the finite coupling time, this method provides a lot of information in a single measurement. For example, the pattern of outcoupled atoms in Fig. 5(b) is curved because the trap frequency changes along the axial direction.

The system studied here is perfectly symmetric. Nevertheless, in any realization of the experiment, the relative phase of the two condensates assumes a specific value and spontaneously breaks the symmetry. The unidirectional

output is equivalent to the magnetization in a ferromagnet, which, by spontaneous symmetry breaking, points into a specific direction. Spontaneous symmetry breaking can be observed in the interference pattern of two overlapping condensates which has a definite phase [18]. Unidirectional output in a symmetric situation more dramatically shows the existence of the condensates' phase.

In conclusion, we experimentally studied the optical coupling between two spatially separate condensates using bidirectional Bragg scattering and demonstrated that the phase of the coupling currents can be controlled. This scheme is a new approach for observing Josephson phenomena, but also for monitoring condensate motion and characterizing trapping potentials.
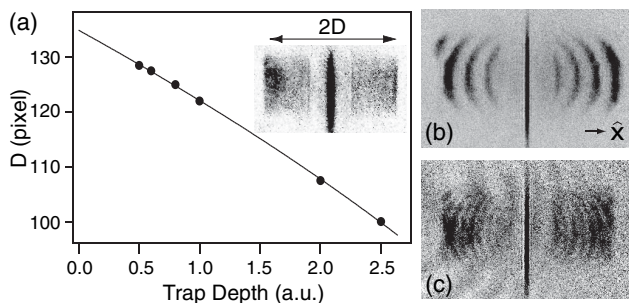
FIG. 5. Trap characterization by continuous outcoupling. (a) Atoms were outcoupled from a single well and the traveling distance D with fixed traveling time $t = 7$ ms was measured, changing the trap depth U by varying the total power of the laser beam forming the single well. The solid line is a fitting curve (see the text for details) with 1 a.u. = 18.0 kHz and 1 pixel = 3.11 μm. Dipole oscillation in the x direction was induced by suddenly shifting the trap center. (b) Outcoupling pattern with Bragg frequency difference $\nu = 2\pi \times 114$ kHz and (c) $\nu = 2\pi \times 101.5$ kHz, which correspond to resonant velocities of ≈ 4 mm/s and ≈ 0 mm/s, respectively. In (b), the left and the right pattern have antisymmetric correlation.

*URL: http://cua.mit.edu/ketterle_group/
[1] B. D. Josephson, Phys. Lett. **1**, 251 (1962).
[2] P. W. Anderson, in *Lectures on The Many-Body Problem*, edited by E. R. Caianiello (Academic, New York, 1964), Vol. 2, pp. 113–135.
[3] P. W. Anderson and J. W. Rowell, Phys. Rev. Lett. **10**, 230 (1963).
[4] S. V. Pereverzev, A. Loshak, S. Backhaus, J. C. Davis, and R. E. Packard, Nature (London) **388**, 449 (1997).
[5] F. S. Cataliotti, S. Burger, C. Fort, P. Maddaloni, F. Minardi, A. Trombettoni, A. Smerzi, and M. Inguscio, Science **293**, 843 (2001).
[6] M. Albiez, R. Gati, J. Fölling, S. Hunsmann, M. Cristiani, and M. K. Oberthaler, Phys. Rev. Lett. **95**, 010402 (2005).
[7] J. Williams, R. Walser, J. Cooper, E. Cornell, and M. Holland, Phys. Rev. A **59**, R31 (1999).
[8] P. Öhberg and S. Stenholm, Phys. Rev. A **59**, 3890 (1999).
[9] A. Imamoglu and T. A. B. Kennedy, Phys. Rev. A **55**, R849 (1997).
[10] J. M. Vogels, J. K. Chin, and W. Ketterle, Phys. Rev. Lett. **90**, 030403 (2003).
[11] M. Saba, T. A. Pasquini, C. Sanner, Y. Shin, W. Ketterle, and D. E. Pritchard, Science **307**, 1945 (2005).
[12] L. Pitaevskii and S. Stringari, Phys. Rev. Lett. **83**, 4237 (1999).
[13] F. Zambelli, L. Pitaevskii, D. M. Stamper-Kurn, and S. Stringari, Phys. Rev. A **61**, 063608 (2000).
[14] Y. Shin, M. Saba, T. A. Pasquini, W. Ketterle, D. E. Pritchard, and A. E. Leanhardt, Phys. Rev. Lett. **92**, 050405 (2004).
[15] A. P. Chikkatur, Y. Shin, A. E. Leanhardt, D. Kielpinski, E. Tsikata, T. L. Gustavson, D. E. Pritchard, and W. Ketterle, Science **296**, 2193 (2002).
[16] V. M. Kaurov and A. B. Kuklov, Phys. Rev. A **71**, 011601(R) (2005).
[17] I. Bouchoule, physics/0502050.
[18] M. R. Andrews, C. G. Townsend, H.-J. Miesner, D. S. Durfee, D. M. Kurn, and W. Ketterle, Science **275**, 637 (1997).